

# Analyst

Accepted Manuscript



This is an *Accepted Manuscript*, which has been through the Royal Society of Chemistry peer review process and has been accepted for publication.

*Accepted Manuscripts* are published online shortly after acceptance, before technical editing, formatting and proof reading. Using this free service, authors can make their results available to the community, in citable form, before we publish the edited article. We will replace this *Accepted Manuscript* with the edited and formatted *Advance Article* as soon as it is available.

You can find more information about *Accepted Manuscripts* in the [Information for Authors](#).

Please note that technical editing may introduce minor changes to the text and/or graphics, which may alter content. The journal's standard [Terms & Conditions](#) and the [Ethical guidelines](#) still apply. In no event shall the Royal Society of Chemistry be held responsible for any errors or omissions in this *Accepted Manuscript* or any consequences arising from the use of any information it contains.



Analyst

PAPER

## Collision Cross Section Calibrants for Negative Ion Mode Traveling Wave Ion Mobility-Mass Spectrometry

Received 00th January 20xx,  
Accepted 00th January 20xx

Jay G. Forsythe,<sup>a,b</sup> Anton S. Petrov,<sup>a,b</sup> Chelsea A. Walker,<sup>a,b</sup> Samuel J. Allen,<sup>c</sup> Jarrod S. Pellissier,<sup>a,b</sup> Matthew F. Bush,<sup>c</sup> Nicholas V. Hud,<sup>a,b,d</sup> and Facundo M. Fernández<sup>\*a,b,d</sup>

DOI: 10.1039/x0xx00000x

www.rsc.org/

Unlike traditional drift-tube ion mobility-mass spectrometry, traveling-wave ion mobility-mass spectrometry typically requires calibration in order to generate collision cross section (CCS) values. Although this has received a significant amount of attention for positive-ion mode analysis, little attention has been paid for CCS calibration in negative ion mode. Here, we provide drift-tube CCS values for [M-H]<sup>-</sup> ions of two calibrant series, polyalanine and polymalic acid, and evaluate both types of calibrants in terms of the accuracy and precision of traveling-wave ion mobility CCS values that they produce.

### Introduction

Ion mobility-mass spectrometry (IM-MS) has gained popularity in multiple areas of chemical and biochemical research,<sup>1-6</sup> providing insight into gas-phase molecular structure, and increased peak capacity on a millisecond timescale.<sup>7,8</sup> Gas-phase structure can be quantitatively determined in the form of collision cross section (CCS) using traditional drift-tube IM (DTIM), as the number of low-energy collisions between an ion and neutral buffer gas molecules in an electrostatic drift tube is proportional to ion size. As a result, drift time can be directly converted to ion-neutral CCS via the Mason-Schamp equation

$$\Omega = \frac{(18\pi)^{1/2}}{16} \frac{ze}{(k_B T)^{1/2}} \left[ \frac{1}{\mu} \right]^{1/2} \frac{t_d E}{L} \frac{760}{P} \frac{T}{273} \frac{1}{N_0} \quad (1)$$

where  $\Omega$  is CCS (typically reported in  $\text{\AA}^2$  or  $\text{nm}^2$ ),  $ze$  is ion charge,  $k_B$  is the Boltzmann constant,  $T$  is temperature (in K),  $\mu$  is the reduced mass,  $t_d$  is drift time,  $E$  is electric field,  $L$  is the length of the tube,  $P$  is pressure (in Torr), and  $N_0$  is the number density of the drift gas under standard temperature and pressure.<sup>9,10</sup>

In addition to DTIM,<sup>11-16</sup> other IM approaches such as traveling-wave IM (TWIM),<sup>17-20</sup> field-asymmetric waveform ion mobility spectrometry (FAIMS),<sup>21-23</sup> and trapped ion mobility spectrometry (TIMS)<sup>24-25</sup> can also be coupled with MS detection. Several of these approaches have been incorporated into commercially-available instruments, a development that has considerably increased the use of IM-MS. The most popular commercial IM-MS platform uses a high ion transmission TWIM mobility cell. The dynamic electric fields used for separation are not typically compatible with theory underlining the Mason-Schamp equation, which typically prevents direct CCS measurement (see ref. 20 for exception). To overcome this limitation, compounds with known DTIM CCS values are typically used as TWIM-MS CCS calibrants, generating parameters for a modified function that incorporates many elements of the Mason-Schamp equation, as described by Smith *et al.*<sup>26</sup> Briefly, the power function

$$\Omega = \frac{(18\pi)^{1/2}}{16} \frac{ze}{(k_B T)^{1/2}} \left[ \frac{1}{\mu} \right]^{1/2} \frac{760}{P} \frac{T}{273} \frac{1}{N_0} A(t_d)^B \quad (2)$$

<sup>a</sup> NSF/NASA Center for Chemical Evolution

<sup>b</sup> School of Chemistry and Biochemistry, Georgia Institute of Technology, Atlanta, GA 30332-0400. 901 Atlantic Dr. NW, Atlanta, GA, USA. E-mail: facundo.fernandez@chemistry.gatech.edu; Fax: +1 (404) 894-7452; Tel: +1 (404) 385-4432

<sup>c</sup> University of Washington, Department of Chemistry, Box 351700, Seattle, WA 98195-1700

<sup>d</sup> Institute of Bioengineering and Biosciences, Georgia Institute of Technology, Atlanta, GA 30332

† Electronic Supplementary Information (ESI) available: [Excel file containing template for calculating CCS on TWIM instrumentation and TWIM CCS values of oligomer series].

is used, where A and B are constants determined from known DTIM CCS calibrants, and other terms are the same as in the Mason-Schamp equation (1). A number of these terms can be grouped together into the constant A', such that

$$\Omega = ze \left[ \frac{1}{\mu} \right]^{1/2} A'(t_d)^B \quad (3)$$

where A' and B are experimentally-derived, and only ion charge and reduced mass terms remain. When appropriate CCS calibrants are chosen, this method – or a variation of this method – generates CCS values for numerous types of positively-charged analytes with good accuracy compared to DTIM measurements.<sup>4,27-35</sup>

In contrast, negative ion mode TWIM CCS calibration strategies have received little attention to date. However, the use of negative mode in MS-based research appears to be increasing in fields such as metabolomics, glycomics, environmental analysis, and biopolymers, where many analytes of interest are relatively acidic and can be deprotonated during ion generation. Moreover, it has been shown that methods which explore both negatively-charged and positively-charged analytes provide a more comprehensive molecular 'snapshot' of a system.<sup>36-38</sup> Additionally, CCS values can be used for feature identification in addition to tandem MS and LC retention time matching.<sup>39</sup> Therefore, it is expected that more researchers will progressively incorporate TWIM separations into negative-mode MS and LC-MS workflows (e.g., HILIC<sup>40-42</sup>).

Several TWIM CCS negative ion mode calibrants have been proposed to date, including poly-DL-alanine,<sup>39</sup> polystyrene,<sup>43-44</sup> dextran,<sup>45</sup> and phosphate clusters.<sup>46</sup> However, for polystyrene and phosphate clusters, experimental DTIM CCS values have not yet been obtained. Thus, these series cannot be readily used as TWIM CCS calibrants at this time. Dextran has been shown to be a good TWIM CCS calibrant for oligosaccharides, but appears to be somewhat fragile in the gas phase. Therefore, we introduce a new CCS calibrant for negative ion mode analysis of small molecules, poly-L-malic acid, which we cross-validate against poly-DL-alanine (Fig. 1) TWIM results based upon absolute DTIM CCS measurements in He and N<sub>2</sub> drift gases. Both of these series ionize well in negative ion mode and demonstrate excellent fitting characteristics for TWIM CCS calibration. Additionally, experimental and computational methods are used to gain insight into gas-phase conformations of the calibrants.

## Experimental

### Materials

Ultra-pure deionized water (18.2 MΩ cm) was generated on a Barnstead Nanopure Diamond system. Poly-DL-alanine (Sigma-Aldrich USA) was prepared at a concentration of 0.01 mg mL<sup>-1</sup> in DI water, into which a dialanine (Bachem Bioscience) solution was spiked in order to better cover low-CCS analytes. L-malic acid monomer was obtained from Chem-Impex International. Poly-L-aspartic acid sodium salt (Alamanda Polymers) was dissolved in DI water at a concentration of 1.4 mg mL<sup>-1</sup>. This solution was then hydrolyzed in 1M HCl at 37°C overnight to shorten the peptides, reconstituted in DI water, and diluted accordingly. L-lactic acid powder (Sigma-Aldrich USA) was polymerized using the same method as for L-malic acid.

### Poly-L-malic Acid Synthesis

L-malic acid monomer (0.050 M in 200 μL of DI water) was placed in an open 1mL Eppendorf container and heated at 85°C for 24 hours to remove water and to drive ester bond formation. After 24 hours, 200 μL of DI water were re-added and subsequently diluted 1:100 to yield 20 mL of 0.50 mM total malic acid. When not being used, samples were stored at -20°C to minimize ester hydrolysis. However, one may also dry-down hydrolyzed samples overnight in order to re-form oligoesters.

### DTIM Analysis

All DTIM measurements were performed using a Waters Synapt G2 HDMS equipped with a 7 mm i.d. RF-confining drift cell.<sup>47</sup> RF-confining drift cells enable accurate CCS measurements without drift time calibration.<sup>27,30,32,47-48</sup> CCS values were determined by measuring drift times at 8 different drift voltages ranging from 125 to 350 V at either 1.5 Torr N<sub>2</sub> or 2 Torr He buffer gas. Reported DTIM CCS values are averages of three replicate experiments performed on separate days.

### TWIM Analysis and Calibration

Analytes were directly infused into a Synapt G2 HDMS platform (Waters Corp., Milford, MA) using electrospray ionization in negative ion mode. Nitrogen was the neutral buffer gas for all TWIM experiments. Instrument settings were as follows: capillary voltage, 2.0 kV; cone voltage, 30 V; extraction cone voltage, 3.0 V; source temperature, 90°C; desolvation temperature, 250°C; cone gas flow, 20.0 L hr<sup>-1</sup>; desolvation gas flow, 650 L hr<sup>-1</sup>; source gas flow, 0.0 mL min<sup>-1</sup>; trap gas flow, 2.0 mL min<sup>-1</sup>; He cell gas flow, 180.0 mL min<sup>-1</sup>; IMS gas flow, 90.0 mL min<sup>-1</sup>; IMS wave delay, 450 μs; IMS wave velocity, 650 m s<sup>-1</sup> or 750 m s<sup>-1</sup>; IMS wave amplitude, 40 V; IMS (N<sub>2</sub>) pressure, 3.67 mbar (2.75 Torr); Transfer wave velocity, 190 m s<sup>-1</sup>; Transfer wave amplitude, 4.0 V; TOF resolution mode (m/Δm = 20,000).

## Analyst

Arrival time distributions were extracted from DriftScope 2.1 and MassLynx 4.1 into OriginPro 9.0 and fit with Gaussian functions to more accurately determine peak maxima. All arrival times were then corrected using the equation

$$t_d' = t_d - \left[ \left( \frac{EDC \text{ delay}}{1000} \right) * \sqrt{m/z} \right] \quad (4)$$

such that the effective drift time ( $t_d'$ ) represented mass-independent flight time through the mobility region (T-wave and transfer). Calibrant DTIM CCS values were normalized according to the function

$$\Omega' = \frac{\Omega}{\left( z * \left[ \frac{1}{\mu} \right]^{1/2} \right)} \quad (5)$$

where  $\Omega'$  is normalized CCS,  $\Omega$  is DTIM CCS (in  $\text{\AA}^2$ ),  $z$  is absolute value of ion charge state, and  $\mu$  is reduced mass.<sup>4</sup> To generate calibration curves,  $t_d'$  and  $\Omega'$  were fit in Origin using Belehradek power functions of the form

$$\Omega = A' * (t_d' - t_0)^B * z \quad (6)$$

where  $t_0$  accounts for the mobility independent contributions to the measured arrival times.<sup>49</sup> This type of fit was found to generate more accurate CCS values than a simple power function of the form  $\Omega = A' * (t_d')^B$ , especially for low-molecular-weight analytes. Reported TWIM CCS values are averaged over five replicate experiments.

### Molecular Dynamics and MOBCAL Simulations

Atomic models were generated using SYBYL-X Suite (2012). Oligomers of alanine and malic acid were initially constructed as ideal  $\alpha$ -helices and were then allowed to fold into new conformations. Malic acid structures were manually derived from the corresponding aspartic acid structures by editing the corresponding PDB files. For each alanine oligomer, a negative charge of 1 was placed on the C-terminal carboxylic acid, maintaining the neutrality of the N-terminus. In contrast, because malic acid oligomers have ionizable side chains, oligomers of the same length were generated containing different deprotonation sites. Specifically, the negative charge was placed at one of the three locations: i) the side chain of the N-terminal residue, ii) the side chain of a central residue, and iii) the C-terminal residue. The AMBER FF99 force field<sup>50</sup> was used for alanine oligomers. The General AMBER force field (GAFF)<sup>51</sup> was used for malic acid and its oligomers; parameters were assigned using the Antechamber<sup>52</sup> package within the AMBER Toolkit. The BCC option was used to assign the charges for Molecular Dynamics (MD) calculations.<sup>53</sup> To generate conformations, 5000 steps of the steepest decent minimization were followed in by 50 ns MD simulations performed in the gas phase at 300 K and a time step of 1 fs using NAMD<sup>54</sup> for malic acid and Gromacs<sup>55</sup> for alanine. Fifty conformations separated by 1 ns were extracted from each MD trajectory using the VMD package.<sup>56</sup> One representative structure from each MD trajectory was re-optimized at the B3LYP/6-31++G(d,p) level of theory using Gaussian.<sup>57</sup> The Projection Approximation method was used to compute CCS.<sup>58</sup> MOBCAL, originally produced by the Jarrold research group, is freely available software for estimating CCS and found at <http://www.indiana.edu/~nano/software.html>.<sup>59,60</sup>

## Results and Discussion

### Polyalanine and Polymalic Acid

The utility of poly-DL-alanine as a TWIM CCS calibrant has been previously discussed in the context of positive-ion mode experiments.<sup>32</sup> Briefly, commercially-available poly-DL-alanine provides a large number of calibration points ( $n=3-14$  for singly-charged species), good fitting characteristics, and high stability to hydrolysis.

To our knowledge, polymalic acid not been used previously for TWIM CCS calibration purposes. Consistent with our previous report on malic acid oligomerization in a prebiotic chemistry context,<sup>61</sup> a solution of malic acid monomer placed in an open container and dried overnight at 85°C resulted in ester bond formation. The oligomers produced in this reaction can be clearly observed by both MS and TWIM analysis (Fig. 2a, b).

Polymalic acid was investigated as an alternative TWIM CCS calibrant for several reasons. Initially, we observed that the relationship between mass-to-charge and arrival time was highly linear (Fig. 2b, inset). Additionally, L-malic acid monomer is very inexpensive (approximately \$1/gram at present), easy to polymerize (Methods), highly soluble in water, and enantiomerically-pure. Although polyester backbones are easier to form than peptide backbones, they are also easier to break, as they are susceptible to hydrolysis - especially in solutions with acidic or basic pH. Nevertheless, we observed that polymalic acid, when dissolved in pH-unadjusted DI water and stored at -20°C, is stable for up to one month before requiring re-polymerization by oven drying.

### Cross-validation of TWIM CCS Calibration by DTIM CCS Values

DTIM CCS values for the [M-H]<sup>-</sup> species of polyalanine and polymalic acid, obtained in both He and N<sub>2</sub> neutral buffer gases, are provided in Table 1 and plotted in Figure 3. It was observed that polymalic acid presented systematic differences with polyalanine in both N<sub>2</sub> and He drift gases, therefore suggesting differences in their interactions with the drift gas, or intrinsically-different structural characteristics. Molecular dynamics and MOBCAL calculations were performed to generate gas-phase conformations and their corresponding CCS values to match those found in experiments. Helium was chosen for these simulations as it is much less polarizable than N<sub>2</sub>, and therefore simpler to use from a computational perspective. Overall, computationally-generated polyalanine CCS values (in He) were found to be in very good agreement with experimental CCS values when the Projection Approximation was used (Table 1).

Unlike polyalanine, which in its [M-H]<sup>-</sup> form is likely deprotonated at the C-terminus,<sup>62</sup> it is not straightforward to predict where malic acid oligomers are deprotonated as every residue side chain has a carboxylic acid moiety. Although specific deprotonation sites were assigned before MD simulations, there may be a mixture of deprotonation sites for oligomers of the same size. Additionally, deprotonation sites may migrate similar to the mobile proton model for positively-charged peptides in the literature.<sup>63</sup> As a result, theoretical CCS errors for polymalic acid were typically greater than those for polyalanine, especially for *n*=4-7 (Table 1). For the *n*=8 oligomer, varying the site of deprotonation did not significantly affect structure, as a number of hydrogen bonds generate the fold (vide infra). However, for intermediately-sized oligomers (e.g., *n*=4-5) stabilized by only a few hydrogen bonds, moving the charge led to large variance in theoretical CCS. For these intermediately-sized oligomers, we also tried generating conformations via Gaussian, although no significant improvements in theoretical CCS were observed. For this reason, efforts are currently underway to optimize charge distributions for polymalic acid and plan to be addressed in subsequent work.

In order to cross-validate both calibrant series, DTIM CCS values of polyalanine were used as calibrants to estimate TWIM CCS values of polymalic acid, and vice versa. Experimental comparisons between DTIM and TWIM CCS were done in N<sub>2</sub> due to the fact that analyte-ion rollover is inefficient in He, which is the fundamental basis for separation in TWIM.<sup>19,64</sup> Initially, ln *t*<sub>d</sub>' vs. ln Ω' curves were used for TWIM calibration (Fig. S1, ESI), which demonstrated good fitting characteristics (R<sup>2</sup> > 0.9998). Using these TWIM calibration functions, CCS values for the opposite chemical series were generated and compared to DTIM CCS values. All TWIM CCS values matched DTIM CCS values within ± 2.0 % error, and 16 of the 20 species matched within ± 1.0 % error (Table S1, ESI). However, we observed a small yet systematic bias in the measurements, which we attribute to this type of calibration not accounting for mobility-independent flight times outside of the traveling-wave mobility cell. For this reason, we decided to use Belehadek power functions to generate our calibration curves (Fig. 4), which gave R<sup>2</sup> values of greater than 0.9999. When these functions were used, all TWIM CCS and DTIM CCS values matched within ± 1.0% error, including low-molecular-weight species (Table 1). Although both sets of CCS values matched very closely, we did observe that the majority of TWIM CCS values were slightly less than their corresponding DTIM CCS values.

Consistent with previous CCS calibration studies in positive ion mode, we observed that the precision for these measurements was typically better than the accuracy, especially for larger species (Table 1).<sup>32, 34, 35</sup> When mobility peaks were fit using Gaussian functions, error in determining peak maxima was minimized and the main sources of variance were likely slight variations in TWIM cell pressure (N<sub>2</sub>) and in room temperature. Nevertheless, all relative standard deviations (RSDs) were less than 0.5 %, and the majority of RSDs were less than 0.2 %.

#### Minimizing Sources of Error in TWIM CCS Calibration

Studies in positive ion mode have previously explored causes of absolute error (bias) in TWIM measurements, and suggested the main cause being calibrant-analyte structural mismatch.<sup>27,28,32,48</sup> To explore if this was true for negative ion mode experiments as well, we compared CCS values of leucine enkephalin (YGGFL) and selected metabolites<sup>39</sup> using both polyalanine and polymalic acid calibration functions (Table 2). All differences in CCS between the two calibrants were less than ± 1.0 %.

Although minor, CCS differences observed between the two calibrants may be attributed to effects related to gas-phase structure. We initially suspected that mobility differences between polyalanine and polymalic acid could be assigned to differences in interactions of the involved ionic species with the somewhat-polarizable N<sub>2</sub> drift gas. However, as shown in Figure 3, differences between polyalanine and polymalic acid in N<sub>2</sub> are consistent with those observed in He, which is less polarizable. Therefore, polyalanine and polymalic acid differences are not artifacts related to elasticity in ion-N<sub>2</sub> collisions but are instead structural by nature.

In order to probe these structural differences further, we obtained TWIM CCS values for lactic acid and aspartic acid (Table S2-S3, ESI), structural analogs of the calibrants used which vary only by the linkage in their polymer backbones. Polylactic acid is the α-hydroxy acid (ester-linked) analog of polyalanine, and polyaspartic acid is the α-amino acid (amide-linked) analog to polymalic acid. CCS values of polyalanine, polylactic acid, polyaspartic acid, and polymalic acid are shown in Figure 5. Polyalanine and polylactic acid show essentially no difference in CCS, and polyaspartic acid and polymalic acid show only minor differences in CCS.

Previous IM studies have shown that some peptides are able to form stable secondary structures in the gas-phase based upon backbone amide hydrogen bonding.<sup>65-71</sup> However, as our calibrants primarily cover the low *m/z* range, linkages of the

*Analyst*

polymer backbones play less of a role in determining gas-phase conformations than do the identity of the residue side chains (-CH<sub>3</sub> for alanine and lactic acid; -CH<sub>2</sub>COOH for aspartic acid and malic acid). Thus, structural differences between polyalanine and polymalic acid are believed to result from not only differences in density<sup>72</sup> but also strong intramolecular hydrogen bonding from the acidic side chain of polymalic acid, consistent with molecular dynamics simulations (Fig. 6).

From these results, it appears that absolute TWIM CCS error in negative mode is primarily caused by structural differences between calibrant and analyte. For positive ion mode, it has been shown that error due to charge-state mismatch (ca. 5 %) is greater than error due to structural mismatch (ca. 1 %, consistent with our data).<sup>34</sup> Calibration error due to charge-state mismatch likely exists in negative mode as well, although it is not applicable to the [M-H]<sup>-</sup> species considered here.

**General Calibration Strategies**

Based on the studies presented here, both polyalanine and polymalic acid appear to be viable negative ion mode CCS calibrants for multiple types of molecules. In contrast with previously-suggested calibrants, these oligomers can be electrosprayed directly from water, ionize well as [M-H]<sup>-</sup> species, demonstrate excellent fitting characteristics, and cover a significant m/z and CCS range for small molecules. Polyalanine is more stable to hydrolysis and generates a wider calibration range than polymalic acid; for these reasons, it is more suitable for long-term, large-scale -omics studies (proteomics, metabolomics, etc.). On the other hand, polymalic acid is easy to prepare, is very soluble in water, is produced from single enantiomer (L-form), and is equally suitable for structural analysis of negatively-charged analytes under 1 kDa. In particular, the strong intramolecular hydrogen bonding of polymalic acid suggests it is an ideal calibrant for acidic and/or polar compounds. Nevertheless, it is possible that researchers will encounter analytes which are structurally dissimilar from both polyalanine and polymalic acid calibrants, and thus would need to find alternative TWIM CCS calibrants for determining gas-phase conformations.

Typically, researchers infuse leucine enkephalin peptide (YGGFL) through the reference electrospray capillary in order to correct for shifts in m/z calibration during LC-TWIM-MS experiments. Lietz et al. suggested that CCS calibrants such as polyalanine could be continuously infused via the Lockspray capillary present on the TWIM-MS instrument platform.<sup>35</sup> This idea is intriguing, as CCS could be corrected in real-time during LC-TWIM-MS acquisitions in a similar manner. Either polyalanine or polymalic acid would be used first in order to generate a multi-point calibration curve, which could then be multiplied by a correction factor based on drift in the observed leucine encephalin CCS.

**Conclusion**

In summary, both polyalanine and polymalic acid have been shown to be appropriate and versatile calibrants for negative-ion mode TWIM CCS determination. Absolute errors for TWIM CCS values were all less than ± 1.0 % when compared to DTIM CCS values. Only minor differences were observed when switching between the two calibrants, due to inherent structural differences in their gas-phase conformations and propagation via calibrant-analyte mismatch. Based on these insights, we project absolute errors of 0.5-1.0 % are to some degree inevitable when generating CCS values on TWIM instrumentation.

**Acknowledgements**

The authors thank Professors Martha A. Grover, F. Joseph Schork (Georgia Institute of Technology), and Ramanarayanan Krishnamurthy (The Scripps Research Institute) for fruitful discussions. This work was supported by the NSF and the NASA Astrobiology Program under the NSF Center for Chemical Evolution [CHE-1004570]. S.J.A. was supported by the American Chemical Society, Division of Analytical Chemistry Fellowship, sponsored by Agilent Technologies.

## References

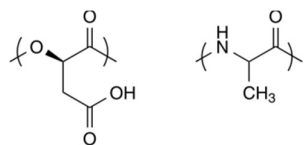
- 1 T. Wytenbach and M. T. Bowers, *Top. Curr. Chem.*, 2003, **225**, 207-232.
- 2 S. Trimpin and D. E. Clemmer, *Anal. Chem.*, 2008, **80**, 9073-9083.
- 3 J. A. McLean, B. T. Ruotolo, K. J. Gillig and D. H. Russell, *Int. J. Mass Spectrom.*, 2005, **240**, 301-315.
- 4 B. T. Ruotolo, J. L. Benesch, A. M. Sandercock, S. J. Hyung and C. V. Robinson, *Nat. Protoc.*, 2008, **3**, 1139-1152.
- 5 D. J. Weston, R. Bateman, I. D. Wilson, T. R. Wood and C. S. Creaser, *Anal. Chem.*, 2005, **77**, 7572-7580.
- 6 S. N. Jackson, M. Ugarov, T. Egan, J. D. Post, D. Langlais, J. Albert Schultz and A. S. Woods, *J. Mass Spectrom.*, 2007, **42**, 1093-1098.
- 7 B. T. Ruotolo, K. J. Gillig, E. G. Stone and D. H. Russell, *J. Chromatogr. B*, 2002, **782**, 385-392.
- 8 B. T. Ruotolo, J. A. McLean, K. J. Gillig and D. H. Russell, *J. Mass Spectrom.*, 2004, **39**, 361-367.
- 9 E. A. Mason and E. W. McDaniel, *Transport Properties of Ions in Gases*, John Wiley & Sons, New York, NY, 1988.
- 10 J. A. McLean, J. A. Schultz and A. S. Woods, in *Electrospray and MALDI Mass Spectrometry: Fundamentals, Instrumentation, Practicalities, and Biological Applications, 2nd Edition*, ed. R. B. Cole, John Wiley & Sons, Hoboken, NJ, 2010, ch. 12, pp. 411-439.
- 11 E. W. McDaniel, W. S. Barnes and D. W. Martin, *Rev. Sci. Instrum.*, 1962, **33**, 2-7.
- 12 G. von Helden, T. Wytenbach and M. T. Bowers, *Int. J. Mass Spectrom.*, 1995, **146**, 349-364.
- 13 D. E. Clemmer and M. F. Jarrold, *J. Mass Spectrom.*, 1997, **32**, 577-592.
- 14 S. C. Henderson, S. J. Valentine, A. E. Counterman and D. E. Clemmer, *Anal. Chem.*, 1999, **71**, 291-301.
- 15 K. Tang, A. A. Shvartsburg, H. N. Lee, D. C. Prior, M. A. Buschbach, F. M. Li, A. V. Tolmachev, G. A. Anderson and R. D. Smith, *Anal. Chem.*, 2005, **77**, 3330-3339.
- 16 J. C. May, C. R. Goodwin, N. M. Lareau, K. L. Leaprot, C. B. Morris, R. T. Kurulugama, A. Mordehai, C. Klein, W. Barry, E. Darland, G. Overney, K. Imatani, G. C. Stafford, J. C. Fjeldsted and J. A. McLean, *Anal. Chem.*, 2014, **86**, 2107-2116.
- 17 K. Giles, S. D. Pringle, K. R. Worthington, D. Little, J. L. Wildgoose and R. H. Bateman, *Rapid Commun. Mass Spectrom.*, 2004, **18**, 2401-2414.
- 18 S. D. Pringle, K. Giles, J. L. Wildgoose, J. P. Williams, S. E. Slade, K. Thalassinou, R. H. Bateman, M. T. Bowers and J. H. Scrivens, *Int. J. Mass Spectrom.*, 2007, **261**, 1-12.
- 19 A. A. Shvartsburg and R. D. Smith, *Anal. Chem.*, 2008, **80**, 9689-9699.
- 20 K. Giles, J. L. Wildgoose, D. J. Langridge and I. Campuzano, *Int. J. Mass Spectrom.*, 2010, **298**, 10-16.
- 21 R. W. Purves, R. Guevremont, S. Day, C. W. Pipich and M. S. Matyjaszczyk, *Rev. Sci. Instrum.*, 1998, **69**, 4094-4105.
- 22 A. A. Shvartsburg, K. Q. Tang and R. D. Smith, *Anal. Chem.*, 2004, **76**, 7366-7374.
- 23 R. Guevremont, *J. Chromatogr. A*, 2004, **1058**, 3-19.
- 24 F. A. Fernandez-Lima, D. A. Kaplan, J. Seutering and M. A. Park, *Int. J. Ion Mobil. Spectrom.*, 2011, **14**, 93-98.
- 25 J. A. Silveira, M. E. Ridgeway and M. A. Park, *Anal. Chem.*, 2014, **86**, 5624-5627.
- 26 D. P. Smith, T. W. Knapman, I. Campuzano, R. W. Malham, J. T. Berryman, S. E. Radford and A. E. Ashcroft, *Eur. J. Mass Spectrom.*, 2009, **15**, 113-130.
- 27 M. F. Bush, Z. Hall, K. Giles, J. Hoyes, C. V. Robinson and B. T. Ruotolo, *Anal. Chem.*, 2010, **82**, 9557-9565.
- 28 W. B. Ridenour, M. Kliman, J. A. McLean and R. M. Caprioli, *Anal. Chem.*, 2010, **82**, 1881-1889.
- 29 Y. Y. Zhong, S. J. Hyung and B. T. Ruotolo, *Analyst*, 2011, **136**, 3534-3541.
- 30 I. Campuzano, M. F. Bush, C. V. Robinson, C. Beaumont, K. Richardson, H. Kim and H. I. Kim, *Anal. Chem.*, 2012, **84**, 1026-1033.
- 31 R. Chawner, B. McCullough, K. Giles, P. E. Barran, S. J. Gaskell and C. E. Eyers, *J. Proteome Res.*, 2012, **11**, 5564-5572.
- 32 M. F. Bush, I. Campuzano and C. V. Robinson, *Anal. Chem.*, 2012, **84**, 7124-7130.
- 33 K. Pagel and D. J. Harvey, *Anal. Chem.*, 2013, **85**, 5138-5145.
- 34 A. S. Gelb, R. E. Jarratt, Y. T. Huang and E. D. Dodds, *Anal. Chem.*, 2014, **86**, 11396-11402.
- 35 C. B. Lietz, Q. Yu and L. J. Li, *J. Am. Soc. Mass Spectrom.*, 2014, **25**, 2009-2019.
- 36 M. Yuan, S. B. Breitkopf, X. M. Yang and J. M. Asara, *Nat. Protoc.*, 2012, **7**, 872-881.
- 37 K. Schuhmann, R. Almeida, M. Baumert, R. Herzog, S. R. Bornstein and A. Shevchenko, *J. Mass Spectrom.*, 2012, **47**, 96-104.
- 38 S. Boudah, M. F. Olivier, S. Aros-Calt, L. Oliveira, F. Fenaille, J. C. Tabet and C. Junot, *J. Chromatogr. B*, 2014, **966**, 34-47.
- 39 G. Paglia, J. P. Williams, L. Menikarachchi, J. W. Thompson, R. Tyldesley-Worster, S. Halldórsson, O. Rólfsson, A. Moseley, D. Grant, J. Langridge, B. O. Palsson and G. Astarita, *Anal. Chem.*, 2014, **86**, 3985-3993.
- 40 Y. Yamaguchi, W. Nishima, S. Re and Y. Sugita, *Rapid Commun. Mass Spectrom.*, 2012, **26**, 2877-2884.
- 41 Q. Ma, G.-C. Xi, C. Wang, H. Bai, Q. Zhang, H.-W. Xi, Z.-M. Wang and L.-H. Guo, *Int. J. Mass Spectrom.*, 2012, **315**, 31-39.
- 42 A. G. M. Leijdekkers, J.-H. Huang, E. J. Bakx, H. Gruppen and H. A. Schols, *Carbohydr. Res.*, 2015, **404**, 1-8.
- 43 J. V. Hamilton, J. B. Renaud and P. M. Mayer, *Rapid Commun. Mass Spectrom.*, 2012, **26**, 1591-1595.
- 44 A. M. Rashid, G. Saalbach and S. Bornemann, *Rapid Commun. Mass Spectrom.*, 2014, **28**, 191-199.
- 45 J. Hofmann, W. B. Struwe, C. A. Scarff, J. H. Scrivens, D. J. Harvey and K. Pagel, *Anal. Chem.*, 2014, **86**, 10789-10795.
- 46 H. Lavanant, V. Tognetti and C. Afonso, *J. Am. Soc. Mass Spectrom.*, 2014, **25**, 572-580.
- 47 S. J. Allen, A. M. Schwartz, M. F. Bush, *Anal. Chem.*, 2013, **85**, 12055-12061.
- 48 R. Salbo, M. F. Bush, H. Naver, I. Campuzano, C. V. Robinson, I. Pettersson, T. J. D. Jorgensen and K. F. Haselmann, *Rapid Commun. Mass Spectrom.*, 2012, **26**, 1181-1193.
- 49 K. Richardson, personal communication.
- 50 J. Wang, P. Cieplak, and P. A. Kollman, *J. Comput. Chem.*, 2000, **21**, 1049-1072.
- 51 J. Wang, R. M. Wolf, J. W. Caldwell, P. A. Kollman and D. A. Case, *J. Comput. Chem.*, 2004, **25**, 1157-1174.
- 52 J. Wang, W. Wang, P. A. Kollman and D. A. Case, *J. Mol. Graphics Modell.*, 2006, **25**, 247-260.
- 53 A. Jakalian, D. B. Jack and C. I. Bayly, *J. Comput. Chem.*, 2002, **23**, 1623-1641.
- 54 J. C. Phillips, R. Braun, W. Wang, J. Gumbart, E. Tajkhorshid, E. Villa, C. Chipot, R. D. Skeel, L. Kalé, and K. Schulten, *J. Comput. Chem.*, 2005, **26**, 1781-1802.
- 55 D. van der Spoel, E. Lindahl, B. Hess, G. Groenhof, A. E. Mark and H. J. Berendsen, *J. Comput. Chem.*, 2005, **26**, 1701-1718.
- 56 W. Humphrey, A. Dalke and K. Schulten, *J. Mol. Graphics*, 1996, **14**, 33-38.

## Analyst

- 1  
2  
3  
4  
5  
6  
7  
8  
9  
10  
11  
12  
13  
14  
15  
16  
17  
18  
19  
20  
21  
22  
23  
24  
25  
26  
27  
28  
29  
30  
31  
32  
33  
34  
35  
36  
37  
38  
39  
40  
41  
42  
43  
44  
45  
46  
47  
48  
49  
50  
51  
52  
53  
54  
55  
56  
57  
58  
59  
60
- 57 M. J. Frisch et al. Gaussian, Inc.: Wallingford, CT, 2009.  
58 G. von Helden, M.-T. Hsu, N. Gotts and M. T. Bowers, *J. Phys. Chem.*, 1993, **97**, 8182-8192.  
59 M. F. Mesleh, J. M. Hunter, A. A. Shvartsburg, G. C. Schatz and M. F. Jarrold, *J. Phys. Chem.* 1996, **100**, 16082-16086.  
60 A. A. Shvartsburg and M. F. Jarrold, *Chem. Phys. Lett.*, 1996, **261**, 86-91.  
61 I. Mamajanov, P. J. MacDonald, J. Ying, D. M. Duncanson, G. R. Dowdy, C. A. Walker, A. E. Engelhart, F. M. Fernández, M. A. Grover, N. V. Hud and F. J. Schork, *Macromolecules*, 2014, **47**, 1334-1343.  
62 S. S. Bokatzian-Johnson, M. L. Stover, D. A. Dixon and C. J. Cassady, *J. Phys. Chem. B*, 2012, **116**, 14844-14858.  
63 V. H. Wysocki, G. Tsapralis, L. L. Smith and L. A. Breci, *J. Mass Spectrom.*, 2000, **35**, 1399-1406.  
64 J. C. May and J. A. McLean, *Int. J. Ion Mobil. Spectrom.*, 2013, **16**, 85-94.  
65 R. R. Hudgins and M. F. Jarrold, *J. Am. Chem. Soc.*, 1999, **121**, 3494-3501.  
66 B. S. Kinnear and M. F. Jarrold, *J. Am. Chem. Soc.*, 2001, **123**, 7907-7908.  
67 A. E. Counterman and D. E. Clemmer, *J. Am. Chem. Soc.*, 2001, **123**, 1490-1498.  
68 A. E. Counterman and D. E. Clemmer, *J. Phys. Chem. B*, 2002, **106**, 12045-12051.  
69 M. F. Jarrold, *Phys. Chem. Chem. Phys.*, 2007, **9**, 1659-1671.  
70 L. J. Morrison and V. H. Wysocki, *J. Am. Chem. Soc.*, 2014, **136**, 14173-14183.  
71 A. R. Johnson, J. M. Dilger, M. S. Glover, D. E. Clemmer and E. E. Carlson, *Chem. Comm.*, 2014, **50**, 8849-8851.  
72 L. S. Fenn, M. Kliman, A. Mahsut, S. R. Zhao and J. A. McLean, *Anal. Bioanal. Chem.*, 2009, **394**, 235-244.

PAPER

Analyst



Poly-L-malic acid

Poly-DL-alanine

**Fig. 1.** Oligomers used for negative ion mode TWIM CCS calibration. Poly-L-malic acid was formed by drying down an aqueous solution of L-malic acid monomer overnight (Methods). For the alanine series, dialanine (L-form) was added to poly-DL-alanine.

Analyst

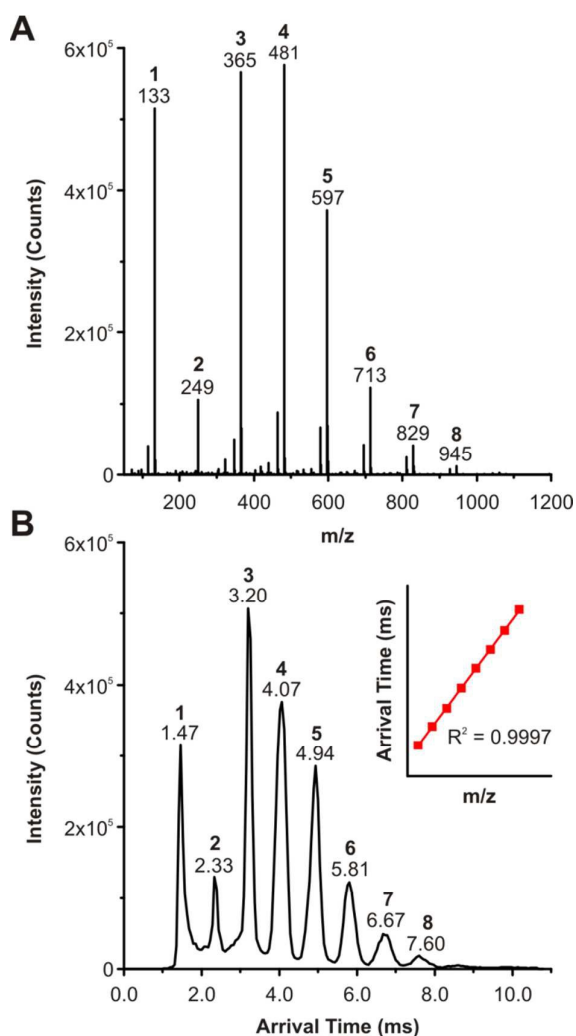


**Fig. 2** MS and TWIM analysis of polymeric acid. (a) Negative-ion mode electrospray mass spectrum. A concentration of 0.50 mM (initial monomer) was infused at  $5 \mu\text{L min}^{-1}$ . Oligomers  $n=1-8$  are detected as  $[\text{M}-\text{H}]^-$  ions and labeled by their  $m/z$  values. (b) TWIM separation based on oligomer size ( $n=1-8$  labeled by their uncorrected arrival times). Traveling wave velocity =  $650 \text{ m s}^{-1}$ ; wave amplitude = 40 V. (Inset) Mass-to-charge and arrival time exhibit an excellent linear relationship.

PAPER

Analyst

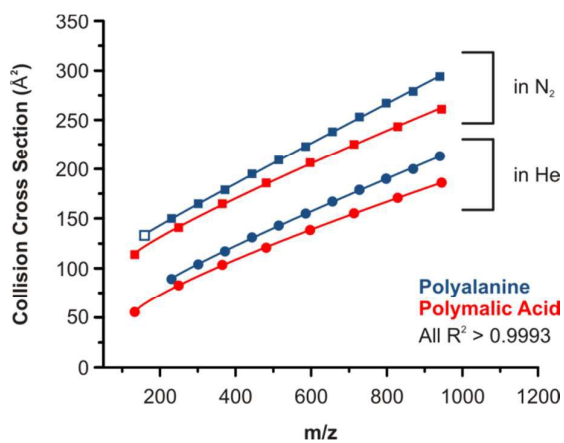


**Fig. 3** Polymalic acid (red) and polyalanine (blue) CCS values in both N<sub>2</sub> (squares) and He drift gases (circles). CCS values are DTIM (filled symbols) except for dialanine which was obtained using TWIM calibration (open symbol). Mass-to-charge vs. CCS curves were fit in Origin using power functions.

Analyst

Calibrant	m/z	DTIM CCS (He)	MOBCAL CCS (He)	% Diff. (MOBCAL:DTIM)	DTIM CCS (N <sub>2</sub> )	TWIM CCS (N <sub>2</sub> , cross-cal.)	% Diff. (TWIM:DTIM)
(Ala) <sub>2</sub>	159.08					132.2 ± 0.1	
(Ala) <sub>3</sub>	230.11	89	93	+4.5%	150.8	150.0 ± 0.5	-0.53%
(Ala) <sub>4</sub>	301.15	104	106	+1.9%	165.5	164.4 ± 0.2	-0.66%
(Ala) <sub>5</sub>	372.19	117	120	+2.6%	180.6	179.7 ± 0.2	-0.50%
(Ala) <sub>6</sub>	443.23	131	132	+0.8%	196.2	195.0 ± 0.2	-0.61%
(Ala) <sub>7</sub>	514.26	143	147	+2.8%	210.3	209.5 ± 0.2	-0.38%
(Ala) <sub>8</sub>	585.30	155	159	+2.6%	223.7	222.4 ± 0.1	-0.58%
(Ala) <sub>9</sub>	656.34	167	166	-0.6%	238.5	237.1 ± 0.1	-0.59%
(Ala) <sub>10</sub>	727.37	179	179	+0.0%	252.8	251.1 ± 0.2	-0.67%
(Ala) <sub>11</sub>	798.41	190			266.0	264.8 ± 0.1	-0.45%
(Ala) <sub>12</sub>	869.45	200			278.2	277.2 ± 0.2	-0.36%
(Ala) <sub>13</sub>	940.49	213			292.8	291.6 ± 0.3	-0.41%
(Ala) <sub>14</sub>	1011.52	226			308*	305.7 ± 0.3	-0.75%
(MA) <sub>1</sub>	133.01	56			113.9	114.3 ± 0.8	+0.35%
(MA) <sub>2</sub>	249.02	83	87	+4.8%	141.0	140.0 ± 0.5	-0.71%
(MA) <sub>3</sub>	365.03	103	109	+5.8%	164.9	163.9 ± 0.4	-0.61%
(MA) <sub>4</sub>	481.04	121	133	+9.9%	185.9	184.5 ± 0.3	-0.75%
(MA) <sub>5</sub>	597.06	138	151	+8.6%	206.3	204.5 ± 0.4	-0.87%
(MA) <sub>6</sub>	713.06	155	164	+5.8%	225.1	224.0 ± 0.4	-0.49%
(MA) <sub>7</sub>	829.08	171	179	+4.7%	243.2	242.6 ± 0.3	-0.25%
(MA) <sub>8</sub>	945.08	186	188	+1.1%	260.9	260.9 ± 0.3	+0.00%

**Table 1.** Experimental and theoretical CCS values of polyalanine and polymalic acid. Cross-validation of polyalanine and polymalic acid calibrants was done by comparing TWIM and DTIM CCS measurements. Polyalanine TWIM values were obtained by using polymalic acid as the calibrant, and polymalic acid TWIM values were obtained by using polyalanine as the calibrant (n=5 measurements). All differences between TWIM and experimental DTIM (N<sub>2</sub>) values are less than ±1.0 %. CCS values are reported in Å<sup>2</sup> and m/z values correspond to [M-H]<sup>-</sup> ions. MOBCAL CCS values were obtained for He drift gas using the Projection Approximation. \*The alanine 14-mer N<sub>2</sub> DTIM CCS value was obtained from reference 39.

PAPER

Analyst

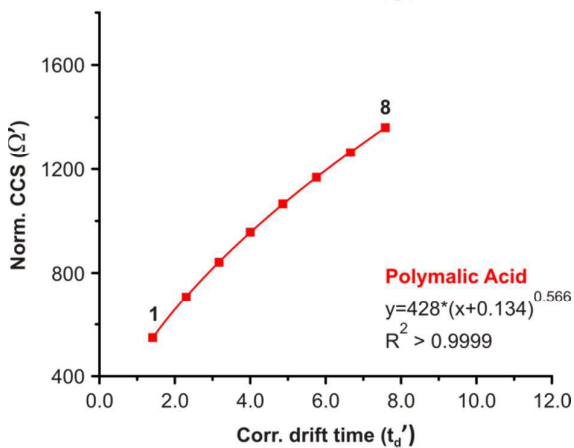
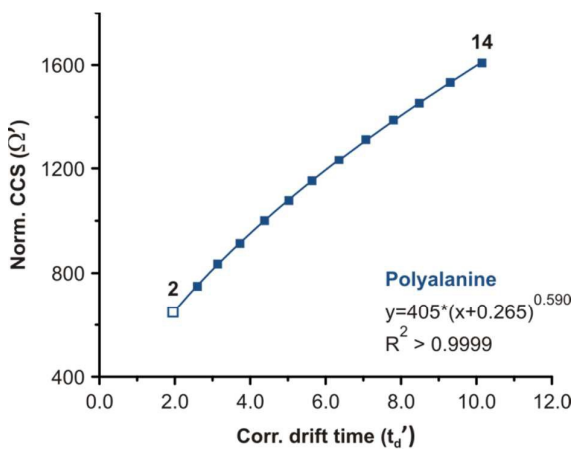


**Fig. 4** TWIM CCS calibration plots for polyalanine ( $n=2-14$ , blue) and polymalic acid ( $n=1-8$ , red) in  $N_2$  drift gas. Normalized CCS values ( $\Omega'$ ) correspond to CCS values in  $\text{\AA}^2$  (all DTIM except for dialanine, unshaded) divided by both charge state and the inverse square root of reduced mass. Corrected drift times ( $t_d'$ ) correspond to mass-independent flight times. The  $t_d'$  vs.  $\Omega'$  curves were fit in Origin using Belehradek power functions.

Analyst

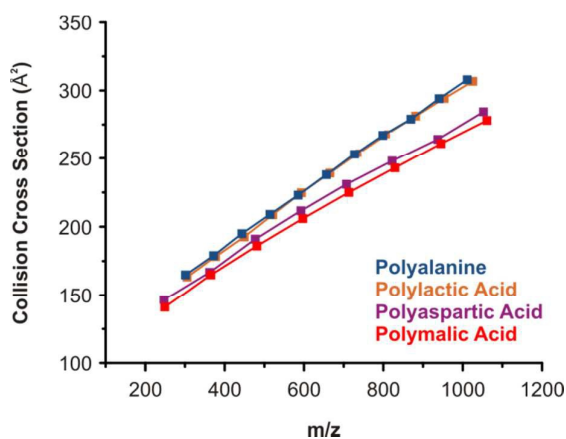


**Fig. 5** Intramolecular hydrogen bonding by malic acid side chains causes compact gas-phase conformations. TWIM CCS values for polyalanine (blue), polylactic acid (orange), polyaspartic acid (purple), and polymalic acid (red) are shown for  $N_2$  drift gas. Polyalanine and polylactic acid differ only by amide/ester linkages, as do polyaspartic acid and polymalic acid. Only minimal differences in structure between these two polypeptides and their polyester analogs are observed. Therefore, conformational differences between polyalanine and polymalic acid are due primarily to different residue side chains ( $-CH_3$  for alanine and  $-CH_2COOH$  for malic acid), and less so to intramolecular hydrogen bonding involving the backbone. TWIM CCS values of polylactic acid and polyaspartic acid  $[M-H]^-$  ions can be found in the Electronic Supplemental Information (Table S2-S3).

PAPER

Analyst

Analyte	m/z	TWIM CCS (N <sub>2</sub> , PolyA cal.)	SD	TWIM CCS (N <sub>2</sub> , PolyMA cal.)	SD	% Diff. (MA:A)
Leucine Enkephalin	554.26	219.4	0.6	219.6	0.1	0.06%
Leucine	130.09	127.7	0.6	127.3	0.1	-0.32%
Salicylic Acid	137.02	117.1	0.7	116.2	0.2	-0.73%
Glutamic Acid	146.05	121.3	0.6	120.7	0.2	-0.51%
Citric Acid	191.02	125.5	0.5	125.2	0.1	-0.27%
Glucuronic Acid	193.03	128.8	0.4	128.6	0.1	-0.16%
UMP	323.03	157.1	0.4	157.6	0.2	+0.32%
AMP	346.06	168.4	0.4	169.0	0.2	+0.36%
ADP	426.02	180.2	0.4	180.8	0.2	+0.35%

**Table 2.** TWIM CCS measurement of leucine enkephalin and several selected metabolites (n=3 measurements for leucine enkephalin; n=5 measurements for metabolites). Leucine enkephalin (YGGFL) is commonly used as the Lockspray real-time m/z calibrant. CCS differences of less than  $\pm 1.0\%$  are observed between the two calibrant sets. CCS values are reported in  $\text{\AA}^2$  and m/z values correspond to  $[\text{M-H}]^-$  ions.

Analyst

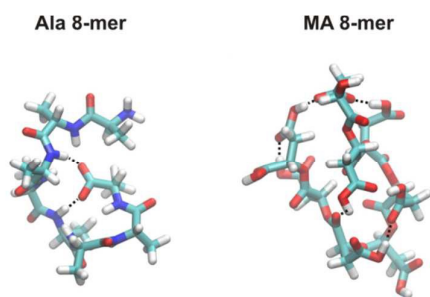


**Fig. 6** Representative structural conformations of alanine (left) and malic acid (right) octamers generated from MD simulations. Malic acid folds tightly due to an increased number of hydrogen bonds. For both oligomers, theoretical CCS values generated using MOBCAL match closely to experimental DTIM CCS values in He drift gas ( $159 \text{ \AA}^2$  MOBCAL vs.  $155 \text{ \AA}^2$  DTIM for Ala 8-mer;  $188 \text{ \AA}^2$  MOBCAL vs.  $186 \text{ \AA}^2$  DTIM for MA 8-mer).